DOI: 10.6060/mhc245998n

Antimicrobial Photodynamic Therapy Activity Properties of 2,6-Brominated and -Iodinated BODIPY Core Dyes and Their -Extended 3,5-Distyryl Analogues

Akwesi Ndundu,[a] Nthabeleng R. Molupe,[b] Azole Sindelo,[b] Lohohola Osomba,[a] Malongwe K'Ekuboni,[a] Bokolombe P. Ngoy,[ab@] John Mack,[b@] and Tebello Nyokong[b]

[a]*Département de Chimie, Université de Kinshasa, B.P. 190 KIN XI, Democratic Republic of the Congo.*
[b]*Institute of Nanotechnology Innovation, Rhodes University, Makhanda 6140, South Africa*
[†]*These authors contributed equally.*
[@]*Corresponding authors E-mail: bokolombe@gmail.com, j.mack@ru.ac.za*

The photodynamic antimicrobial chemotherapy (PACT) activity properties of 2,6-dibrominated and -diiodinated meso-methyl phenyl ester BODIPY dyes π-extended with 3,5-p-dibenzyloxystyryl groups at the 3,5-positions were investigated against Gram-(+) Staphylococcus aureus and Gram-(−) Escherichia coli bacteria and Candida albicans fungus using LEDs with output maxima at 660 and 530 nm. The core dyes were found to have significantly higher PACT activities than the π-extended dyes in the context of the Gram-(+) and -(−) bacterial strains, while low PACT activity was also observed against Candida albicans with the 2,6-dibrominated core dye. The results are consistent with the trends reported in a previous study with BODIPY core and 3,5-divinylene dyes and provide further evidence that research related to the PACT activity properties of BODIPYs should focus primarily on halogenated core dyes. The use of a methyl-β-cyclodextrin inclusion complex was found to significantly enhance the aqueous solubility and PACT activity of the 2,6-diiodinated with 3,5-p-dibenzyloxystyryl groups at the 3,5-positions.

Keywords: BODIPYs, photophysics, TD-DFT calculations, photodynamic antimicrobial chemotherapy.

Антимикробные свойства и фотодинамическая активность 2,6-бромированного и йодированного BODIPY и их π-расширенных 3,5-дистириловых аналогов

Аквеси Ндунду,[a] Нтабеленг Р. Молупе,[b] Азол Синдело,[b] Лохохола Осомба,[a] Малонгве К'Экубони,[a] Боколомбе П. Нгой,[ab@] Джон Мак,[b@] Тебелло Ниоконг[b]

[a]*Департамент Химии, Университет Киншасы, Б.П. 190 КИН XI, Демократическая Республика Конго.*
[b] *Институт инноваций в области нанотехнологий, Университет Родса, Маханда 6140, Южная Африка*
†Эти авторы внесли равный вклад.
[@]*E-mail: bokolombe@gmail.com, j.mack@ru.ac.za*

Свойства фотодинамической антимикробной химиотерапии (PACT) 2,6-дибромированных и -дийодированных мезо-метилфенилэфирных красителей BODIPY, π-расширенных с 3,5-п-дибензилоксистириловыми группами в 3,5-положениях, были исследованы против бактерий Gram-(+) Staphylococcus aureus и Gram-(−) Escherichia coli, а также грибка Candida albicans с использованием светодиодов с выходными максимумами при 660 и 530 нм. Было обнаружено, что основные красители имеют значительно более высокую активность PACT, чем π-расширенные красители в контексте штаммов бактерий Gram-(+) и -(−), в то время как низкая активность PACT также наблюдалась против Candida albicans с 2,6-дибромированным основным красителем. Результаты согласуются с тенденциями, о которых сообщалось в предыдущем исследовании с ядром BODIPY и 3,5-дивиниленовыми красителями, и предоставляют дополнительные доказательства того, что ис-

следования, связанные со свойствами активности PACT BODIPY, должны быть сосредоточены в первую очередь на галогенированных красителях ядра. Было обнаружено, что использование комплекса включения метил-β-циклодекстрина значительно повышает растворимость в воде и активность PACT 2,6-дииодированных с 3,5-п-дибензилоксистириловыми группами в 3,5-положениях.

Ключевые слова: BODIPY, фотофизика, расчеты TD-DFT, фотодинамическая антимикробная химиотерапия.

Introduction

The emergence of bacterial strains that are resistant to common antibiotics provides a challenge to researchers in identifying alternative antibacterial treatments.[1] Photodynamic antimicrobial chemotherapy (PACT) involves a photosensitizer (PS) dye, molecular dioxygen, and light of an appropriate wavelength is among the methods which has been shown to provide promising results *in vitro* and *in vivo*.[2-5] Electron or energy transfer from the triplet state of the PS dye to molecular dioxygen results in the generation of reactive oxygen species (ROS) *via* Type I and Type II reactions, respectively, which deactivate the bacteria. Boron dipyrromethene (BODIPY) dyes were selected as the PS dyes of interest in this study (Scheme 1). They were first reported by Treibs and Kreuzer in 1968,[6] and in recent years have become the focus of considerable research interest for many applications, including use as laser dyes,[7] as nonlinear optical material,[8,9] as fluorescent switches[10] and as chemosensors.[11] The synthesis of BODIPY derivatives is straightforward due to the versatility of BODIPY core dyes for facilitating further functionalization. The introduction of halogen atoms to the 2,6-positions of the BODIPY core can significantly enhance the rate of intersystem crossing, resulting in relatively high singlet oxygen quantum yields, making the dyes potentially suitable for anticancer and antibacterial photodynamic therapy.[12,13]

Recently, we reported a study that demonstrated that the *meso*-aryl ring introduced into the structure of 2,6-brominated core dyes can have a very significant effect on their PACT activity properties against *Staphylococcus aureus* (*S. aureus*).[13] *Meso*-(*p*-methoxycarbonyl)phenyl functionality at the *meso*-carbon in the context of the 2,6-dibrominated core dye **1a** in Scheme 1 was found to significantly enhance the deactivation of this Gram-(+) bacterium. Halogenation of BODIPY dyes enhances the rate of intersystem crossing, including the singlet oxygen, because of the heavy atom effect. In another recent study, we reported that 2,6-halogenated core dyes exhibited enhanced PACT activity relative to 3,5-divinylene dyes.[14] We have previously reported the optical limiting properties of the corresponding π-extended 3,5-*p*-dibenzyloxystyryl dye (**1b**).[15] The bulky *p*-dibenzyloxy groups can hinder π-π stacking in solution. Aggregation can result in less favorable photophysicochemical properties. In this study, we report the PACT activities of this dye against *S. aureus*, *Escherichia coli* (*E. coli*) and *Candida albicans* (*C. albicans*) in comparison to the core dye and its 2,6-diiodinated analogue (**2a**). We also report a study of whether the formation of cyclodextrin inclusion complexes can be used to enhance the PACT activity properties against *S. aureus* of the 2,6-diiodo-3,5-distyryl BODIPY dye with *p*-benzyloxystyryl groups (**2b**). Methyl-β-cyclodextrin (mβCD) was used because of its enhanced aqueous solubility.[16]

Experimental

Materials

2,4-Dimethylpyrrole, methyl 4-formylbenzoate, β-cyclodextrin (βCD), mβCD, trifluoroacetic acid (TFA), *p*-chloranil, triethylamine (TEA), boron trifluoride diethyl etherate, N-bromosuccinimide (NBS), N-iodosuccinimide (NIS), $CDCl_3$, diphenylisobenzofuran (DPBF), Rose Bengal, Rhodamine 6G, zinc phthalocyanine (ZnPc), acetic acid, benzene and piperidine were obtained from Sigma-Aldrich and were used without any further purification with the exception that 2,4-Dimethylpyrrole was distilled before use. Spectroscopic grade dimethylsulfoxide (DMSO) and dimethylformamide (DMF) were supplied by Merck, while dichloromethane (DCM) was obtained from Minema. Tryptic soy broth was purchased from Sigma Aldrich. *E. coli* (ATCC 25922) was purchased from Microbiologic USA, while *C. albicans* (ATCC 24433) and *S. aureus* (ATCC 25923) were obtained from Davies Diagnostics. Agar bacteriological BBL Muller Hinton broth and nutrient agar were purchased from Merck. A phosphate buffer saline (PBS) solution with a solution a pH 7.4 (10 mM PBS) was prepared using appropriate amounts of Na_2HPO_4, KH_2PO_4 and chloride salts dissolved in ultrapure Type II water supplied by an Elga, Veolia water Purelab, flex system (Marlow, UK).

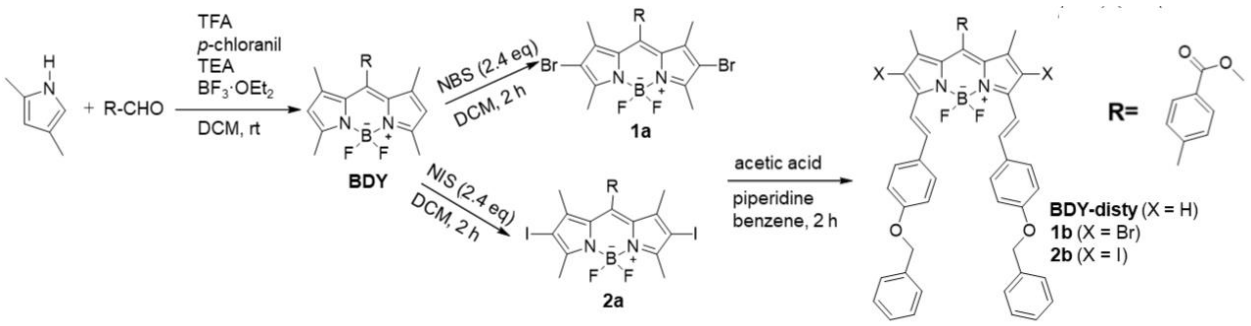

Scheme 1. Synthesis of *meso*-(*p*-methoxycarbonyl)phenyl-substituted BODIPY dyes **BDY**, **1a**, **2a**, **BDY-disty**, **1b** and **2b**.

Equipment

UV-visible absorption spectra were recorded on a Shimadzu UV-2550 spectrophotometer. 1H NMR spectra were recorded on a Bruker 600 MHz spectrometer in $CDCl_3$. Mass spectral data were acquired on a Bruker Auto-FLEX III Smartbeam MALDI-TOF mass spectrometer operated in positive ion mode using α-cyano-4-hydroxycinnamic acid as a matrix. Monochromatic laser light (420–709 nm) from an Ekspla NT 342B-20-AW pulsed laser (2.0 mJ / 5 ns, 20 Hz) was used for quantifying the singlet oxygen quantum yield (Φ_Δ) values of **2a** and **2b** in DMSO with DPBF as a $^1O_2$ quencher and Rose Bengal (Φ_Δ = 0.76 in DMSO)[17] and ZnPc (Φ_Δ = 0.67 in DMSO)[18] as standards. Fluorescence emission spectra were recorded on a Varian Eclipse spectrofluorimeter to determine the fluorescence quantum yield (Φ_F) values of **2a** and **2b** in DMSO by using Rhodamine 6G (Φ_F = 0.95 in ethanol)[19] and zinc phthalocyanine (ZnPc) (Φ_F = 0.20 in DMSO).[20] Laser flash photolysis measurements were used to determine triplet lifetime values and were carried out with an Ekspla NT 342B-20-AW laser containing an Nd:YAG (355 nm, 78 mJ / 7 ns, 20 Hz) pumping a 420−2300 nm range optical parametric oscillator (8 mJ / 7 ns, 20 Hz) to provide the pump beam for an Edinburgh Instruments LP980 instrument fitted with a PMT-LP (Hamamatsu R928P) for kinetic measurements and an ICCD camera (Andor DH320T-25F03) for transient absorption spectroscopy. Bubbling with argon for 15 min was used to deaerate the solutions. The dyes were excited close to the maxima of the main BODIPY spectral bands of **1a**, **1b**, **2a** and **2b**. Thermogravimetric analysis (TGA) was conducted using a Perkin-Elmer TGA 7 analyzer.

Synthesis

The synthesis of the non-halogenated *meso*-(*p*-methoxycarbonyl)phenyl-substituted core dye (BDY), **1a**, the non-halogenated π-extended 3,5-*p*-dibenzyloxystyryl dye (**BDY-disty**) and **1b** (Scheme 1) has been reported previously.[12] Similar procedures were used to prepare **2a** and **2b** by using NIS rather than NBS[16,17] followed by a modified Knoevenagel condensation method.[21,22]

*2,6-Diiodo-1,3,5,7-tetramethyl-8-meso-(p-methoxycarbonyl)phenylBODIPY (**2a**).* **BDY** (0.5293 g, 1.385 mmol) was dissolved in 30 ml dry DCM. The solution was degassed, and 2 eq NIS (0.9347 g, 4.155 mmol) in DCM (5 ml) was added dropwise over 30 min with stirring. The reactions then proceeded for 8 h (monitored by TLC). The solution was washed with a 1 M sodium thiosulfate solution, and the product was extracted with DCM. The extracted product solution was filtered through anhydrous $MgSO_4$ and then dried *in vacuo*. The products were isolated by silica column chromatography with 1:4 ethyl acetate/hexane (v/v) used as the eluent. **2a** was obtained as a dark pink crystalline product in 78% yield. ^{1}H NMR ($CDCl_3$, 293 K) δ_H ppm: 8.23 (d, J = 6.0 Hz, 2H), 7.41 (d, J = 6.0 Hz, 2H), 4.01 (s, 3H), 2.67 (s, 6H), 1.39 (s, 6H. MALDI-TOF MS: Calculated: 634.01 amu; Found: 635.98 m/z $[M+H]^+$.

*2,6-Diiodo-1,7-dimethyl-3,5-dibenzyloxystyryl-8-meso-(p-methoxycarbonyl)phenylBODIPY (**2b**).* **2a** (0.157 g, 0.2469 mmol) and 3 eq of 4-benzyloxybenzaldehyde (0.1779 g, 0.7406 mmol) were mixed and dissolved in dry benzene (20 ml). Glacial acetic acid (0.85 ml) and piperidine (0.85 ml) were added under reflux, and a Dean-Stark trap was used. The reaction was monitored by UV-visible absorption spectroscopy until **2a** was fully consumed. The mixture was washed with 1 M HCl and dried *in vacuo*. The residue was purified by silica chromatography using petroleum 4:1 diethyl ether/ethyl acetate (v/v). **2b** was obtained as a green product in 91% yield. ^{1}H NMR ($CDCl_3$, 293 K) δ_H ppm: 8.24 (d, J = 7.0, 2H), 8.16 (d, J = 16.6, 2H), 7.63 (t, J = 15.1 Hz, 6H), 7.48 (d, J = 6.5, 4H), 7.44 (d, J = 7.3, 6H), 7.37 (d, J = 6.4, 2H), 7.06 (d, J = 7.5, 4H), 5.16 (s, 4H), 4.02 (s, 3H), 1.59 (s, 6H). MALDI-TOF MS: Calculated: 1022.48 amu; Found: 1022.64 m/z $[M]^+$.

*Cyclodextrin inclusion complexes of **2b***

In order to prepare inclusion complexes of **2b** with βCD and mβCD (**2b/βCD** and **2b/mβCD**), thermogravimetric analysis was first used to determine the water content of **2b**, βCD and mβCD as 3%, 13% and 0% respectively. The method used for inclusion complex formation has been described by Miclea *et al.*[23] and Hedges,[24] and was followed with the modifications described in an earlier study we reported on Sn(IV) *meso*-tetraacenaphthylporphyrin.[25] The amount of water in each sample was accounted for by calculating the molar ratios of the dye and cyclodextrin. Since CDs are spectroscopically transparent, UV-visible absorption spectroscopy can be used to determine whether an inclusion complex has formed. The interaction between the dye and mβCD results in significantly enhanced solubility in aqueous media.[13,22] Molar ratios of 1:3 for **2b** to βCD or mβCD were used during the initial complexation. The modified complexation method was adapted from Miclea *et al.*[23] βCD or mβCD was dissolved in a minimum amount of water and heated to 100°C. When the CDs were completely dissolved, **2b** was dissolved in DMSO, since this provided optimal solubilization, and the **2b** solution formed was added gradually. The solution was left to stir for 72 h, then cooled to ambient temperature. The solutions were filtered, and the product was recrystallized in water. The solvents were allowed to evaporate slowly, and the products were stored at room temperature for further use. Thermogravimetric analysis was used to confirm that the inclusion complex was formed in an approximate 1:3 ratio so that PACT activity studies could be carried out in proof of principle terms.

Antimicrobial studies

Antimicrobial activity was assessed using model isolates of *S. aureus*, *E. coli*, and *C. albicans*. The microorganisms were cultured on agar plates following the manufacturer's instructions to obtain individual colonies. Bacterial cultures were prepared according to established procedures.[26,27] Colonies were inoculated into nutrient broth and then placed on a rotary shaker at 200 rpm in an incubator at 37°C overnight to enable bacteria growth. Aliquots of the bacteria culture were transferred into freshly prepared broth (4 mL) and further incubated at 37°C to achieve a mid-logarithmic phase (OD 620 nm ≈ 0.6). The broth culture was removed through centrifugation (3000 rpm for 15 min) for 15 min at 3000 rpm to obtain the bacteria in its mid-logarithmic phase. The bacterial suspension was subsequently centrifuged and washed three times with PBS. The resulting pellet was resuspended in 100 mL of PBS to create a 10^{-2} microorganism suspension stock. Homogenization of bacterial suspension was achieved using the PRO VSM-3 Labplus Vortex mixer. Serial dilutions (10^{-3}, 10^{-4}, 10^{-5}, 10^{-6}, and 10^{-7}) were then prepared for bacterial optimization. From each dilution, 100 µL was aseptically inoculated in triplicate on agar plates, followed by 18 h incubation at 37°C. Colony forming unit (CFU) value counting was performed, and the dilution factor of 10^{-6} was deemed most suitable for this study for all three microorganisms.

PACT activity studies were carried out following a previously reported procedure.[26] For all experiments, microorganism suspensions were incubated for 30 min in an oven with a shaker at 37 °C. 3 ml of the incubated suspension was irradiated at the absorption maxima of the main spectral band of the BODIPY in a 24-well plate. The other 3 ml of *S. aureus* suspension was plated in a 24-well plate and kept in the dark. For photodynamic antimicrobial therapy (PACT), the Thorlabs M660L4 or M530L3 LEDs with output maxima at 660 and 530 nm mounted onto the illumination kit of a Modulight 7710-680 medical laser system to provide a dose of 100 and 39 $mJ \cdot cm^{-2} \cdot min^{-1}$, respectively. During the PACT activity studies against *S. aureus* and *E. coli*, a 5% DMSO/PBS mixture was used to dissolve **1a**, **2a** and **1b**. Solutions of 3.125, 6.25, 12.5, 25, 50, and 100 µM were prepared and exposed to the appropriate light source for 60 min or kept in the

dark, while a similar approach was used for *C. albicans* with 50 and 200 uM solutions of **1a** and **1b**. A 0.5% DMF/PBS mixture was used to dissolve **2b** and **2b/mβCD**. 4.9 μM solutions were used for the PACT activity studies against *S. aureus*, and the appropriate LED was used for 180 min in 45 min intervals. Control experiments were carried out to ensure that the DMSO and DMF used to solubilize the dyes had no significant effect on the microorganisms. Subsequently, 100 μL was inoculated in triplicate on agar plates, followed by 18 h incubation at 37 °C. After photoirradiation, 100 μL samples were inoculated onto agar plates and incubated at 37 °C for 24 h. A similar protocol was followed for the 24 well plates kept in the dark. Bacterial cell harvesting was performed using the Hermle Z233M-2 centrifuge. Bacterial optical density was measured with the Ledetect 96. Colony forming units ($CFU \cdot mL^{-1}$) were evaluated using the Scan® 500 automatic colony.

Theoretical calculations

Optimized geometries were calculated for the *meso*-methylester-substituted 1,3,5,7-tetramethylBODIPY core dye (**BDY**), **1a**, **2a**, the non-brominated 3,5-benzyloxystyrylBODIPY (**BDY-disty**), **1b**, and **2b** at the B3LYP/SDD level of theory by using the Gaussian 09 software package[28] with Grimme's D3 correction for intramolecular repulsion effects.[29] The CAM-B3LYP functional was used for TD-DFT calculations since it contains a long-range correction.

Results and Discussion

Synthesis and characterization

The synthesis and characterization of **BDY**, **1a**, **BDY-disty** and **1b** (Scheme 1) was reported previously in the context of a study on the optical limiting properties of π-extended BODIPY dyes.[12] In this study, similar procedures were used to prepare **2a** and **2b**. The anticipated nineteen and thirty-nine protons for **2a** and **2b**, respectively, can be readily assigned in the ^{1}H NMR spectrum (Figure 1), while the parent peaks observed in the MALDI-TOF MS data match the anticipated structures.

Photophysical properties

Normalized absorption spectra in dichloromethane of the **BDY**, **1a**, **BDY-disty** and **1b** series of dyes that we reported previously in the context of optical limiting studies[15] and those of **BDY**, **2a** and **2b** in DMSO are shown in Figure 2. Photophysical data for **1a**, **1b**, **2a** and **2b** in DMSO are provided in Table 1. There is a large red shift of the main BODIPY spectral band when vinylene groups are added to the 3,5-positions of the BODIPY core (Figure 3). As has been reported previously,[30] the introduction of halogen atoms at the 2,6-positions results in a slight red shift of the main BODIPY spectral band due to the mesomeric effect of the lone pairs on the halogen atoms. The HOMO has larger MO coefficients at these positions than the LUMO (Figure 3). There is hence a smaller stabilization of the HOMO relative to the LUMO in the context of the 2,6-dihalogenated dyes and a slight narrowing of the HOMO−LUMO gaps and a red shift of the main visible region spectral band (Figures 2 and 3A), which is used for photoexcitation during the PACT activity experiments. When vinylene groups are added at the 3,5-positions, there is a large destabilization of the HOMO and a larger narrowing of the HOMO−LUMO gap and red shift of the main spectral band (Figures 2 and 3A). When Grimme's D3 correction is applied, the styryl group lies almost co-planar with the BODIPY core, and the calculated spectra of **1b** and **2b** are almost identical as is also observed experimentally. The Φ_F values in DMSO of **2a** and **2b** were found to be significantly lower than those reported previously for **1a** and **1b** (Table 1),[8,15] due to the heavy atom effect of the iodine atoms introduced at the 2,6-positions.

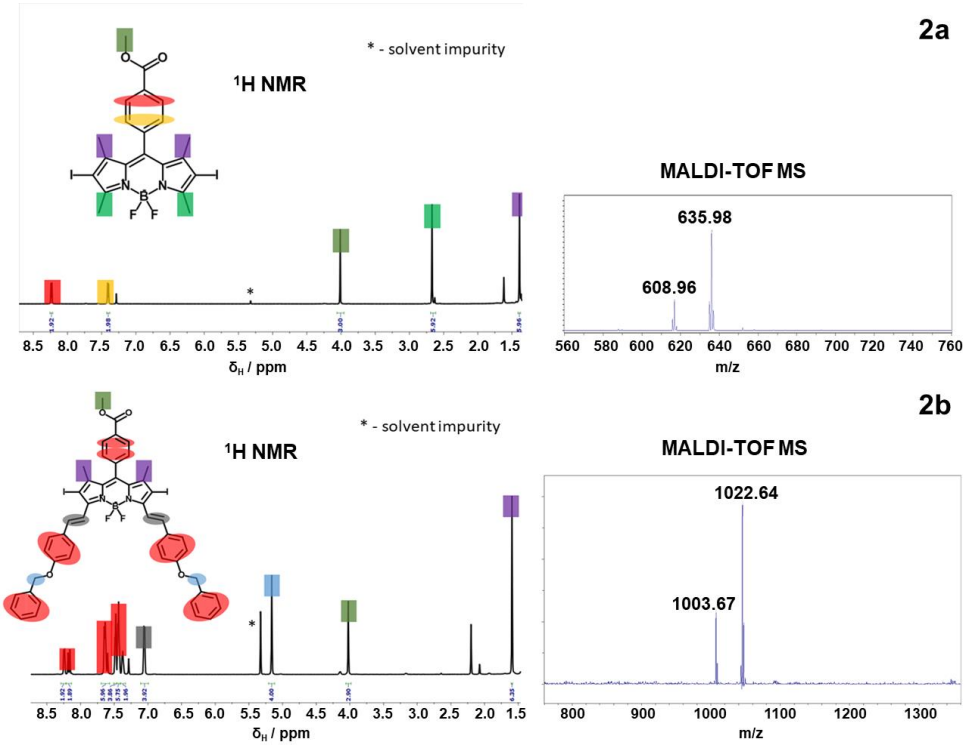

Figure 1. The ^{1}H NMR spectra of **2a** and **2b** in $CDCl_3$ and MALDI-TOF MS data.

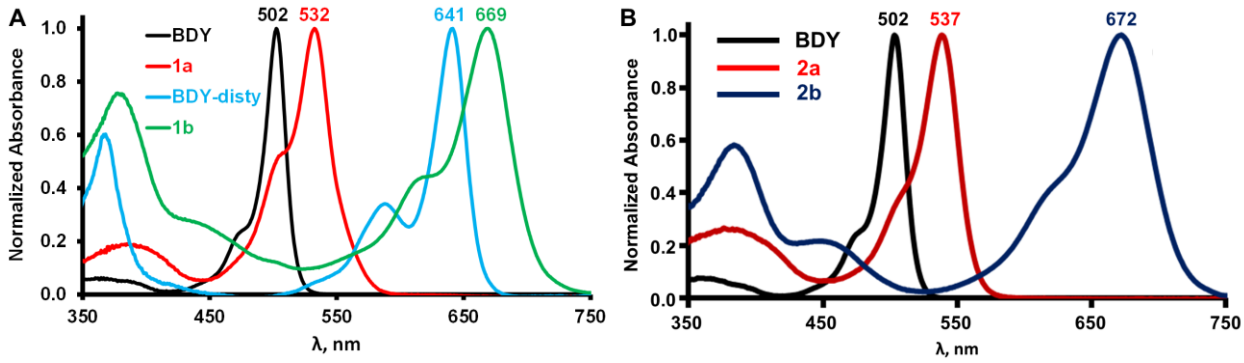

Figure 2. (A) Normalized UV-visible absorption spectra of **BDY**, **1a**, **BDY-disty**, and **1b** in dichloromethane, (B) normalized UV-visible absorption spectra of **BDY**, **2a**, and **2b** in DMSO.

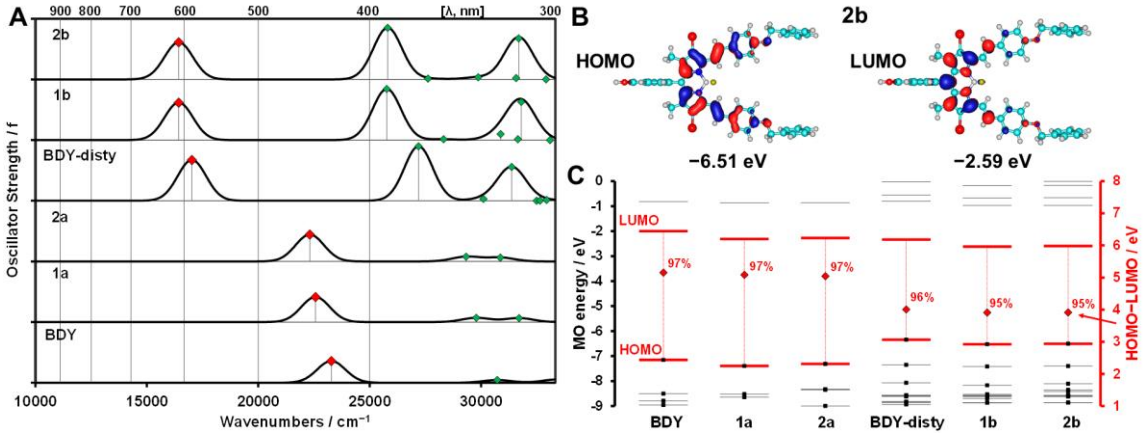

Figure 3. (A) Calculated TD-DFT spectra for **BDY**, **1a**, **2a**, **BDY-disty**, **1b** and **2b** at the CAM-B3LYP/SDD level of theory. The simulated spectra were calculated using Chemcraft at a fixed bandwidth of 1500 cm^{-1}. Red diamonds are used to highlight the main BODIPY spectral band. (B) Angular nodal patterns and MO energies of **2b** at an isosurface of 0.3 a.u. (C) The MO energies of **BDY**, **1a**, **2a**, **BDY-disty**, **1b** and **2b** at the CAM-B3LYP/SDD level of theory. The HOMO and LUMO are highlighted with thick red lines. Black squares denote occupied MOs. Red diamonds highlight HOMO−LUMO gap values plotted against a secondary axis. Percentage values for the contribution of the HOMO → LUMO one-electron transition to the main BODIPY spectral band in (A) are provided next to the red diamonds.

Table 1. Photophysical data for **1a**, **1b**, **2a** and **2b**.

	Solvent	λ_{abs} (nm)[a]	λ_{ex} (nm)[b]	λ_{em} (nm)[c]	Stokes shift (cm^{-1})	Φ_F	Ref.
1a	DMSO	530	530	549	653	0.20	[8]
1b	DMSO	677	677	707	627	0.14	[15]
2a	DMSO	537	537	560	765	0.02	--
2b	DMSO	672	674	707	693	< 0.01	--

[a]The maximum of the main spectral band in the UV-visible absorption spectrum. [b]The maximum of the main spectral band in the fluorescence excitation spectrum. [c]The maximum of the main spectral band in the fluorescence emission spectrum.

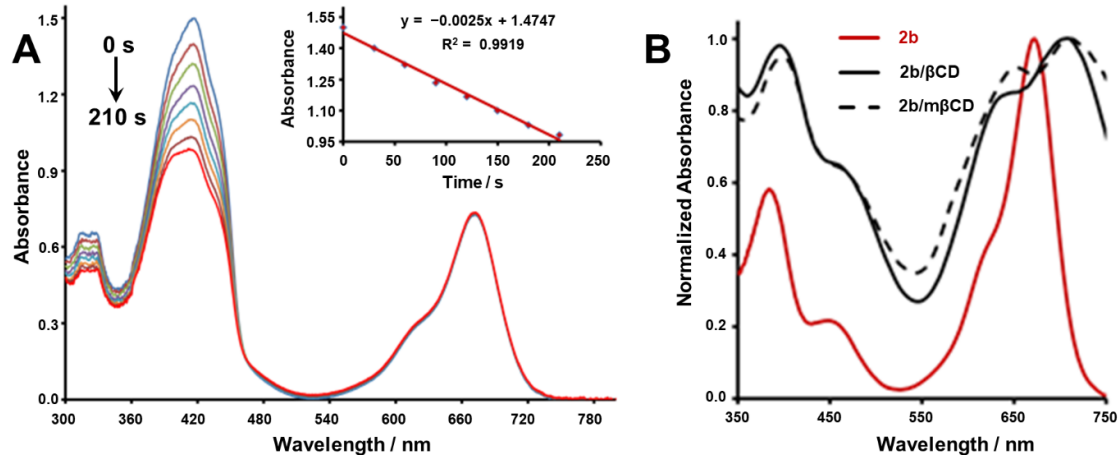

Figure 4. (A) UV-visible absorption spectra in DMSO showing the photodegradation of DPBF in the presence of **2b** at 30 s intervals. The inset provides the change in the absorption values for the DPBF peak at 418 nm over 210 s. (B) UV-visible absorption spectra of **2b** in DMSO, and **2b/βCD** and **2b/mβCD** in water.

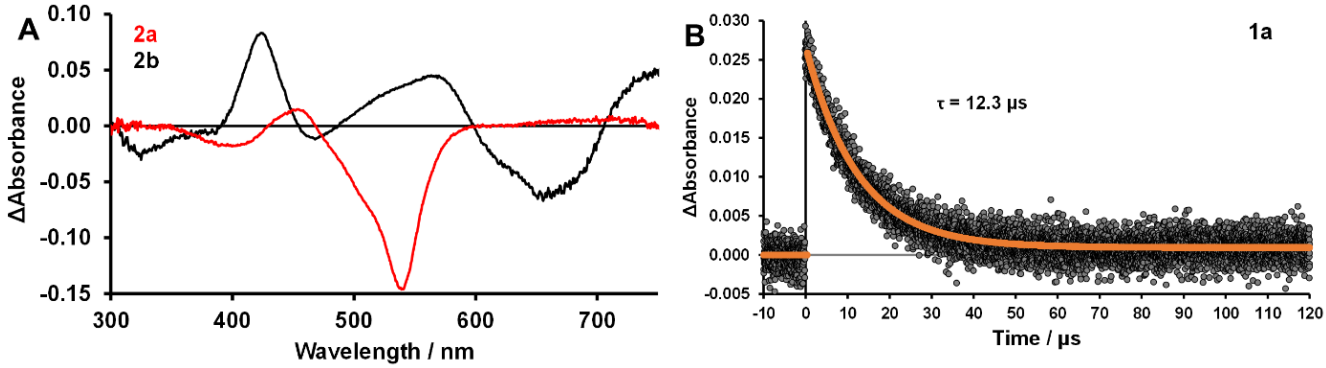

Figure 5. (A) Transient absorption spectra of **2a** and **2b** in DMSO obtained with 7 ns laser pulses at excitation wavelengths of 539 and 672 nm, respectively. (B) The triplet state decay curve measured for **1b** in deaerated DMSO.

Table 2. The singlet oxygen quantum yield and triplet state lifetime (τ_T) values of **1a**, **1b**, **2a** and **2b** in DMSO.

	Solvent	Φ_Δ	Ref.	λ_{ex} (nm)	τ_T (μs)
1a	DMSO	0.40	[8]	500	12.3
1b	DMSO	0.26	--	640	8.2
2a	DMSO	0.63	[15]	539	55.7
2b	DMSO	0.52	--	672	9.4

Table 2. PACT activity data against *S. aureus* after photoirradiation with 530 and 660 nm Thorlabs LEDs.

	Conc. (μM)	Medium	Log_{10} (CFU·mL^{-1})	LED	Time (min)	Dose (J·cm^{-2})	Ref.
1a	1	2% DMSO/PBS	9.66	Thorlabs M530L3	30	1.2	[15]
1b	10	5% DMSO/PBS	1.82	Thorlabs M660L3	60	6.0	--
2b	4.9	0.5% DMF/PBS	0.30	Thorlabs M660L3	180	18.0	--
2b/mβCD	4.9	0.5% DMF/PBS	1.30	Thorlabs M660L3	180	18.0	--

Photochemical studies and laser flash photolysis

The Φ_Δ values of **2a** and **2b** were determined by using DPBF as a $^1O_2$ scavenger (Figure 4, Table 1) and were found to be significantly higher than those of **1a** and **1b**. Laser flash photolysis with 7 ns laser pulses was carried out in deaerated solutions by exciting at the main BODIPY spectral bands. Transient spectra for **2a** and **2b** are provided as examples in Figure 5. We previously reported a femtosecond timescale study with a non-halogenated π-extended 3,5-*p*-dibenzyloxystyryl BODIPY dye with a *meso*-*p*-acetamidophenyl group.[31] Triplet state lifetimes of **1a**, **1b**, **2a** and **2b** were determined to be in the 8.2−55.7 μs range (Figure 5, Table 2) and hence suitable for PACT activity studies.

Antimicrobial studies

The PACT studies for **1a**, **2a**, and **1b** were conducted for 60 min at various concentrations to assess the antimicrobial efficacy of photosensitizers against three microorganisms, namely, Gram-(+) *S. aureus* and Gram-(−) *E. coli* bacteria, and the fungus *C. albicans*. In the context of *S. aureus*, BODIPY core complexes **1a** and **2a** exhibited significantly higher bactericidal effects than **1b** with complete eradication upon photoirradiation of *S. aureus*, even at the lowest concentration used in a manner consistent with what has been reported previously for **1a** (Table 3),[12] so these data sets are not included in Figure 6.

S. aureus is a Gram-(+) bacteria which can be readily photoinactivated by positively charged, negatively charged or neutral photosensitizers, including BODIPYs.[32,33] Neutral photosensitizers such as **1a**, **1b**, **2a** and **2b** can easily penetrate the *S. aureus* cell wall, comprised of a capsule and a thick peptidoglycan layer. Concentration-dependent studies revealed that increasing the concentration of **1b** resulted in an increase in PACT activity, with a percentage reduction of 98.5% at 100 μM (Figure 6). Upon irradiation with a Thorlabs M660L4 LED, the antibacterial activity was significantly enhanced, as reported previously for BODIPY π-extened with thienylvinylene groups at the 3,5-positions.[34] When **2b/βCD** and **2b/mβCD** inclusion complexes were formed (Figure 4), the aqueous solubility of **2b** was significantly enhanced in the case of the latter relative to the former as would normally be anticipated.[16] Enhanced PACT activity was observed for **2b/mβCD** at a lower incubation concentration of 4.9 μM with significantly lower dark toxicity observed relative to **2b** (Figure 6). The limited number of colonies observed after 60 min photoirradiation could be eliminated by increasing the light dose and/or dye concentration. This data set demonstrates in proof of principle terms that the use of the cyclodextrin inclusion complexes of BODIPYs merits further in-depth study.

Similar trends were observed with *E. coli* (Figure 7). Concentration-dependence studies revealed increased PACT activity with an increase in dye concentration. Incubation with core dyes **1a** and **2a** resulted in photoeradication at 25 μM, while significantly lower PACT activity was observed with **1b** with 12% viable cells present even after 1 h irradiation at 100 μM. Gram-(−) bacteria, such as *E. coli*, have a size-exclusion porin outer membrane with inner phospholipid and outer negatively charged lipopolysaccharide membranes, which envelope a thin peptidoglycan layer resulting in an effective permeability barrier which restricts the uptake of many photosensitizer dyes.[35-38] Gram-(−) bacteria are, therefore, inactivated mainly by positively charged photosensitizer dyes that interact with the outer

layer electrostatically, or by dyes that can disrupt the permeability barrier.[35,37,38] Our future studies will focus on dyes with positively charged moieties introduced at the *meso*-aryl and/or other positions on the periphery of the BODIPY core.

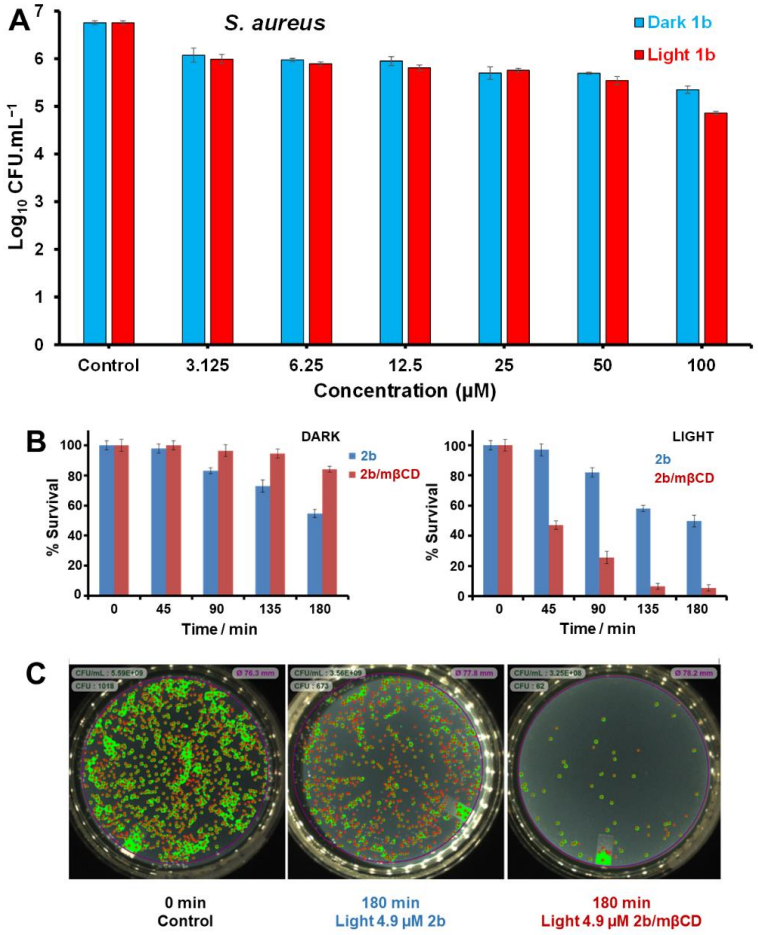

Figure 6. (A) Log_{10} reduction values for **1b** against *S. aureus* in 5% DMSO/PBS after 60 min of irradiation with a Thorlabs M660L4 LED to provide a dose of 6.0 $J \cdot cm^{-2}$ relative to a dark control. (B) Survival percentage for **2b** and **2b/mβCD** in 0.5% DMF/PBS over 180 min of irradiation with a Thorlabs M660L4 LED providing a dose of 100 $mJ \cdot cm^{-2} \cdot min^{-1}$ (LIGHT) against a dark control (DARK). (C) Images of *S. aureus* at the zero control (LEFT), *S. aureus* with **2b** after 180 min irradiation (MIDDLE) and *S. aureus* with **2b/mβCD** at 180 min irradiation (RIGHT) showing the bacteria colonies.

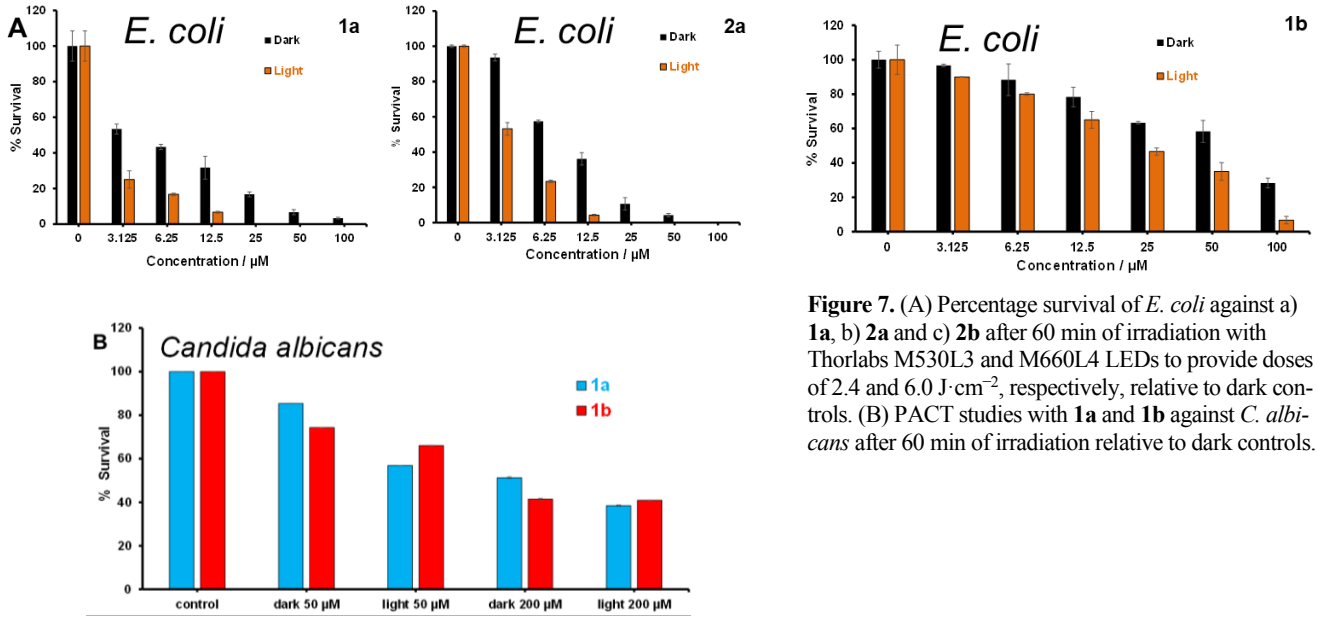

Figure 7. (A) Percentage survival of *E. coli* against a) **1a**, b) **2a** and c) **2b** after 60 min of irradiation with Thorlabs M530L3 and M660L4 LEDs to provide doses of 2.4 and 6.0 $J \cdot cm^{-2}$, respectively, relative to dark controls. (B) PACT studies with **1a** and **1b** against *C. albicans* after 60 min of irradiation relative to dark controls.

PACT activity studies against the fungus *C. albicans* were conducted using concentrations of 50 and 200 μM for **1a** and **1b**. Neither achieved total eradication (Figure 7). This may be due to the fungus possessing a more complex cell morphology than those of *S. aureus* and *E. coli*.[39] A larger phototoxicity effect was observed relative to the dark control in the context of the **1a** core dye despite a lower light dose of 2.4 rather than 6.0 $J \cdot cm^{-2}$ being involved.

Conclusions

The photodynamic antimicrobial chemotherapy (PACT) activity properties of 2,6-dibrominated and -diiodinated BODIPY dyes π-extended with 3,5-*p*-dibenzyloxystyryl groups at the 3,5-positions were investigated against Gram-(+) *S. aureus* and Gram-(−) *E. coli* bacteria and *Candida albicans*. Core dyes **1a** and **2a** were found to have significantly higher PACT activities than the π-extended dyes **1b** and **2b** in the context of the Gram-(+) and -(−) bacterial strains, while low PACT activity was also observed against *Candida albicans* with **1**a and **2a**. The results suggest that research related to the PACT activity properties of BODIPYs should focus primarily on halogenated core dyes rather than their π-extended 3,5-divinylene analogues. The use of a methyl-β-cyclodextrin inclusion complex was found to significantly enhance the aqueous solubility and PACT activity of **2b**. This approach merits further in-depth study.

Acknowledgements. The National Research Foundation (NRF) of South Africa and the Department of Science and Technology (DST) provided financial support through the DST/NRF South African Research Chairs Initiative for Professors of Medicinal Chemistry and Nanotechnology (uid: 62620) to TN and a South Africa-Flanders grant (uid: 119259) to JM. This work was also supported by the Council for Scientific and Industrial Research (CSIR) of South Africa National Laser Centre through the Rental Pool Programme, a CSIR African Laser Centre grant (ALC-R005) to JM and BPN, and by a Pearson-Young Memorial Trust Bursary to NRM. The theoretical calculations were carried out at the Centre for High Performance Computing in Cape Town, South Africa.

Author Contributions. Please, Insert each author's contribution.

References

1. Mamone L., Ferreyra D.D., Gándara L., Di Venosa G., Vallecorsa P., Sáenz D. *J. Photochem. Photobiol. B.* **2016**, *161*, 222–229. DOI: 10.1016/j.jphotobiol.2016.05.026.
2. Xu Z., Gao Y., Meng S., Yang B., Pang L., Wang C., Liu T. *Front. Microbiol.* **2016**, *7*, 242. DOI: 10.3389/fmicb.2016.00242.
3. Liu Y., Qin R., Zaat S.A.J., Breukink E., Heger M. J. Clin. Transl. Res. **2015**, *1*, 140–167. DOI: 10.18053/jctres.2015 03.002.
4. Cieplik, F., Deng, D., Crielaard, W., Buchalla, W., Hellwig, E., Al-Ahmad, A.,Maisch, T. *Crit. Rev. Microbiol.* **2018**, *44*, 571–589. DOI: 10.1080/1040841X.2018.1467876.
5. Youf R., Müller M., Balasini A., Thétiot F., Müller M., Hascoët A., Jonas U., Schönherr H., Lemercier G., Montier T., Le Gall T. *Pharmaceutics* **2021**, *13*, 1995. DOI: 10.3390/pharmaceutics 13121995.
6. Treibs A., Kreuzer F.H. *Justus Liebigs Ann. Chem.* **1968**, *718*, 208–223. DOI: 10.1002/jlac.19687180119.
7. Arbeloa T.L., Arbeloa F.L., Arbeloa I.L., Garcia-Moreno I., Costela A., Sastre R., Amat-Guerri F. *Chem. Phys. Lett.* **1999**, *299*, 315–321. DOI: 10.1016/S0009-2614(98)01281-0.
8. Ngoy B.P., May A.K., Mack J., Nyokong, T. *J. Mol. Struct.* **2019**, *1175*, 745–753. DOI: j.molstruc.2018.08.012.
9. Harris J., May A.K., Ngoy B.P., Mack J., Nyokong, T. *J. Porphyrins Phthalocyanines* **2019**, *23*, 63–75. DOI: 10.1142/S1088424619500019.
10. Trieflinger C., Rurack K., Daub J. *Angew. Chem. Int. Ed.* **2005**, *44*, 2288–2291. DOI: 10.1002/anie.200462377.
11. Gabe Y., Ueno T., Urano Y., Kojima H., Nagano T. *Anal. Biochem.* **2006**, *386*, 621–626. DOI: 10.1007/s00216-006-0587-y.
12. Bomanda B.T., Waudo W., Ngoy B.P., Muya J.T., Mpiana P.T., Mbala M., Openda I., Mack J., Nyokong T. *Macroheterocycles* **2018**, *11*, 429–437. DOI: 10.6060/mhc 180898n.
13. May A.K., Ngoy B.P., Mack J., Nyokong T. *J. Porphyrins Phthalocyanines* **2024**, *28*, 88–96. DOI: 10.1142/S108842 4623501316.
14. Sen P., Sindelo A., Nnaji N., Mack J., Nyokong T. *Photochem. Photobiol.* **2023**, *99*, 947–956. DOI: 10.1111/ php.13698.
15. Ngoy B.P., Hlatshwayo Z., Nwaji N., Fomo G., Mack J., Nyokong T. *J. Porphyrins Phthalocyanines* **2018**, *22*, 413–422. DOI: 10.1142/S1088424617500857.
16. Saokham P., Muankaew C., Jansook P., Loftsson T. *Molecules* **2018**, *23*, 1161. DOI: 10.3390/molecules23051161.
17. Gandra N., Frank A.T., Le Gendre O., Sawwan N., Aebisher D., Liebman J.F., Houk K.N., Greer A., Gao R. *Tetrahedron* **2006**, *62*, 10771−10776. DOI: 10.1016/j.tet. 2006.08.095.
18. Ogunsipe A., Maree D., Nyokong T. *J. Mol. Struct.* **2003**, *650*, 131−140. DOI: 10.1016/S0022-2860(03)00155-8.
19. Fischer M., Georges J. *Chem. Phys. Lett.* **1996**, *260*, 115−118. DOI: 10.1016/0009-2614(96)00838-X.
20. Jiao L., Pang W., Zhou J., Wei Y., Mu X., Bai G., Hao E. *J. Org. Chem.* **2011**, *76*, 9988−9996. DOI: 10.1021/jo201754m.
21. Ngoy B.P., Molupe N., Harris J., Fomo G., Mack J., Nyokong T. *J. Porphyrins Phthalocyanines* **2017**, *21*, 431−438. DOI: 10.1142/S1088424617500420.
22. Zhu S., Zhang J., Vegesna G., Tiwari A., Luo F.-T., Zeller M., Luck R., Li H., Green S., Liu H. *RSC Adv.* **2012**, *2*, 404−407. DOI: 10.1039/C1RA00678A.
23. Miclea L.-M., Vlaia L., Vlaia V., Hădărugă D.I., Mircioiu C. *Farmacia* **2010**, *58*, 583−593.
24. Hedges A.R. *Chem. Rev.* **1998**, *98*, 2035−2044. DOI: 10.1021/cr970014w.
25. Molupe N., Babu B., Prinsloo E., Kaassis A., Edkins K., Mack J., Nyokong T. *J. Porphyrins Phthalocyanines* **2019**, *23*, 1486−1494. DOI: 10.1142/S1088424619501633.
26. Sindelo A., Osifeko O.L., Nyokong T. *Inorg. Chim. Acta* **2018**, *476*, 68−76. DOI: 10.1016/j.ica.2018.02.020.
27. Chavez-Esquivel G., Cervantes-Cuevas H., Ybieta-Olvera L.F., Briones M.C., Acosta D., Cabello, J. *Mater. Sci. Eng. C*, **2021**, *123*, 111934. DOI: 10.1016/j.msec.2021.111934.
28. Gaussian 09, Revision E.01, Frisch M.J., Trucks G.W., Schlegel H.B., Scuseria G.E., Robb M.A., Cheeseman J.R., Scalmani G., Barone V., Mennucci B., Petersson G.A., Nakatsuji H., Caricato M., Li X., Hratchian H.P., Izmaylov A.F., Bloino, J., Zheng, G., Sonnenberg J.L., Hada M., Ehara M., Toyota K., Fukuda R., Hasegawa J., Ishida M., Nakajima T., Honda Y., Kitao O., Nakai H., Vreven T., Montgomery J.A. Jr, Peralta J.E., Ogliaro F., Bearpark M., Heyd J.J., Brothers E., Kudin K.N., Staroverov V.N., Kobayashi R., Normand J., Raghavachari K., Rendell A., Burant J.C., Iyengar S.S., Tomasi J., Cossi M., Rega N., Millam J.M., Klene M., Knox J.E., Cross J.B., Bakken V., Adamo C., Jaramillo J., Gomperts R., Stratmann R.E., Yazyev O., Austin

A.J., Cammi R., Pomelli C., Ochterski J.W., Martin R.L., Morokuma K., Zakrzewski V.G., Voth G.A., Salvador P., Dannenberg J.J., Dapprich S., Daniels A.D., Farkas Ö., Foresman J.B., Ortiz J.V., Cioslowski J., Fox D.J. Gaussian Inc., Wallingford CT, 2009.
29. Grimme S., Antony J., Ehrlich S., Krieg H. *J. Chem. Phys.* **2010**, *132*, 154104. DOI: 10.1063/1.3382344.
30. Lu H., Mack J., Yang Y., Shen Z. *Chem. Soc. Rev.* **2014**, *43*, 4778−4823. DOI: 10.1039/c4cs00030g.
31. Ngoy B.P., May A.K., Mack J., Nyokong T. *Front. Chem.* **2019**, *7*, 740. DOI: 10.3389/fchem.2019.00740.
32. Wardlaw J.L., Sullivan T.J., Lux C.N., Austin F.W. *Vet. J.* **2012**, *192*, 374−377. DOI: 10.1016/j.tvjl.2011.09.007.
33. Ryskova L., Buchta V., Slezak R. *Central Eur. J. Biology* **2010**, *5*, 400–406. DOI: 10.2478/s11535-010-0032-2.
34. Bomanda B.T., Waudo W., Ngoy B.P., Muya J.T., Mpiana P.T., Mbala M., Openda I., Mack J., Nyokong T. *Macroheterocycles* **2018**, *11*, 429–437. DOI: 10.6060/mhc180898n.
35. Ghorbani J., Rahban D., Aghamiri S., Teymouri A., Bahador A. *Laser Ther*. **2018**, *27*, 293–302. DOI: 10.5978/islsm.27_18-RA-01.
36. Sperandio F.F., Huang Y.Y., Hamblin M.R. *Recent Pat. Antiinfect. Drug Discov.* **2013**, *8*, 108–120. DOI: 10.2174/1574891x113089990012.
37. Zgurskaya H.I., López C.A., Gnanakaran S. *ACS Infect. Dis.* **2016**, *1*, 512–522. DOI: 10.1021/acsinfecdis.5b00097.
38. Cieplik F., Deng D., Crielaard W., Buchalla W., Hellwig E., Al-Ahmad A., Maisch T. *Crit. Rev. Microbiol.* **2018**, *44*, 571–589. DOI: 10.1080/1040841X.2018.1467876.
39. Poulain D. *Crit. Rev. Microbiol.* **2015**, *41*, 208–17. DOI: 10.3109/1040841X.2013.813904.

Received 13.07.2024
Accepted 04.10.2024